Journal of the European Ceramic Society 23 (2003) 943–949

www.elsevier.com/locate/jeurceramsoc

R-curve evaluation and bridging stress determination in alumina by compliance analysis

M.E. Ebrahimi*, J. Chevalier, G. Fantozzi

GEMPPM, INSA-Lyon, 69621 Villeurbanne Cedex, France

Received 14 January 2002; received in revised form 14 June 2002; accepted 22 June 2002

Abstract

A procedure is proposed which allows for bridging stress determination and R-curve evaluation from compliance data. R-curves were obtained on the single edge notched beam (SENB) and double torsion (DT) specimens by in situ and direct measurements of crack lengths. The compliance of DT specimens with different successive re-notching and without re-notching was compared. An approach for determining crack bridging stresses of the crack wake from the results of compliance measurements was extended for different grain sizes of alumina ceramics. By this compliance analysis, the K_R- curve of alumina ceramics can be predicted from the compliance function, $\phi(\Delta a)$, versus the crack extension, Δa. The results show that compliance analysis can be a powerful tool for crack bridging stresses evaluation and even for R-curve prediction.

Keywords: Al_2O_3; Bridging stress; Mechanical properties; R-curve; Testing

1. Introduction

Several coarse-grained ceramics show R-curve behavior that is related to grain bridging in the wake of propagation crack. In pure alumina ceramics (>99.8%), an increase in crack resistance with crack extension is often observed.[1–4] It is also well-known that the crack-interface grain 'bridging' behind a crack tip is the major toughening mechanisms in alumina ceramics.[4–7] The sawcut and renotching experiments performed by Knehans and Steinbrech[7] confirm the bridging influence on the crack resistance (R) curve as the initial toughness was recovered after renotching of the extended crack tip.

Various methods are used for determining of R-curves from controlled crack propagation test. The basic difference between these methods is the procedure for measuring the crack length during crack extension. From direct and in-situ measurements of crack length by means of a traveling microscope and recording of load during crack growth, all information is available to calculate stress intensity factor $K_{I\ appl}$. However, R-curves of ceramic materials are very often evaluated from load-displacement curves by the crack lengths obtained indirectly from specimen compliance which increases with increasing crack length. Unfortunately, the crack length resulting from compliance is not correct, especially in case of strong R-curve behavior.[8] It means that the compliance is affected by bridging stress, and this effect obviously is higher for coarse-grained alumina ceramics. The consequences of the bridging interactions on fracture-mechanical considerations may become very serious. In the presence of bridging stresses at the crack faces, deviations in the compliance have to be expected from theoretical considerations.[9]

It is noted that the R-curve behavior of alumina ceramics is not a unique material property. If a crack-interface bridging zone is comparable to the dimensions of specimen,[10] the shape of curve depends on the geometry of the test specimen, the initial crack length, the test method and the type of loading (bending, tension and loading points) and particularly on stable and subcritical crack propagation.[11] By analyzing the geometrical influence upon the R-curve, it can be found that the toughness of alumina can be severely overestimated from a sharply rising R-curve which is due to

* Corresponding author at present address: Department of Ceramic and Materials Engineering, Rutgers University, NJ 08854, USA.
E-mail address: ebrahimi@rci.rutgers.edu (M.E. Ebrahimi).

0955-2219/03/$ - see front matter
PII: S0955-2219(02)00230-3

the limited specimen dimensions.[12] Therefore, simple test methods or obtaining reproducible results for the same material are necessary for analyzing the resistance behavior of ceramics.

Accordingly, the determination of crack-interface bridging stress is essential to understand and predict the crack propagation behavior of alumina ceramics. The bridging stresses are extremely non-linear and their range of extension is not negligible compared with the crack length. Several theories have been developed for determining the bridging stress.[8,13–16] Bridging stresses can be determined with the simplified bridging theory from measurements of unloading compliances as a function of crack growth for monotonically applied stresses. Similar to the crack-wake renotching experiment on alumina, a consecutive sawcut experiments could be performed to remove progressively crack bridges behind a crack tip and evaluate their effects on compliance. Renotching results in an increase in compliance as the crack-tip shielding effect is removed. A compliance-based bridging theory can be developed by using the compliance results obtained from sawcut experiments.

The aim of this study is to determine the bridging-stress distribution in alumina under monotonic loading and to predict the R-curve independent from test conditions. The DT test method was applied for crack bridging-analysis because of more stability in crack propagation results.

2. Experimental method

2.1. Material

The starting materials were a high purity (>99.99 wt.%) alumina powder (AKP50, Sumitomo, Tokyo, Japan) with a particle sizes of 0.1–0.3 μm and an alumina powder (SM8, Baikowski, Paris, France) (>99.9 wt.% purity) with 500 ppm MgO and an average particle size of 0.25 μm.

The powders were uniaxially pressed at 60 MPa and cold isostatically pressed at 350 MPa. The green density was about 55% of theoretical density. The green compacts were sintered at 1550–1750 °C for 2–12 h in air. Grain size and morphology were examined by scanning electron microscopy (SEM) on thermally etched surfaces. The grain size of Al_2O_3 ceramics was obtained by an image analysis on the SEM photomicrographs.

The various sintering conditions and physical properties of different alumina ceramics are listed in Table 1. The code numbers after powder type in this table represent the average grain size after sintering of each alumina.

2.2. SENB Method

The R-curve is determined during crack propagation from the crack resistance K_R as a function of crack length. The four-point geometry was used. The tests were performed with single-edge-notched specimens of size 4×6×42 mm (B×W×L). The specimens were pre-notched to a depth "a_0" so that the ratio a_0/W was chosen between 0.55 and 0.6 with a radius tip of 35 μm to control the stability at the onset of crack propagation. The specimens were loaded in air, in a strain-controlled mode with a constant speed of 3 μm/min.

The crack length was determined by an in situ measurement. The specimens were polished down to 1 μm to observe the crack. The real crack length at the surface of the specimen was observed with an optical microscope with a high focus distance during loading of specimen. Crack propagation was viewed in real time and routinely taped on a video-recording unit for closer study.

2.3. Double torsion method

The double torsion (DT) method was used to study compliance analysis and R-curve determination on pre-cracked specimens. The geometry of the DT specimen, test method and loading configuration can be found in Refs. [17,18]. The dimensions of the DT plates were: length 40 mm, width 20 mm and thickness 2 mm.

Compliance analysis was carried out on DT specimens with different notch lengths (successive notching

Table 1
Sintering conditions and physical properties of alumina ceramics

Code	Sintering conditions	% Theoretical density	Mean grain size (μm)	Shape of grains
AKP6	1550 °C, 2 h	98.6	6.3±2.0	Equiaxed
AKP9	1650 °C, 2 h	98.9	9.1±2.9	Equiaxed
AKP14	1750 °C, 6 h	99.3	14.3±5.4	Equiaxed-elongated
AKP36	1750 °C, 12 h	99.6	35.5±17.8	Elongated
SM4	1550 °C, 2 h	99.2	4.3±1.0	Equiaxed
SM8	1650 °C, 2 h	99.2	7.7±2.0	Equiaxed
SM20	1750 °C, 6 h	99.5	19.6±6.8	Equiaxed

from 10 to 30 mm on the same specimen) for the various grain sizes of alumina ceramics. The results were compared with those obtained by natural crack growth (without renotching) for the same alumina.

R-curves were also measured with the DT technique on pre-cracked specimens. Load -deflection curves, with a series of loading-unloading sequences to follow crack extension, were measured at a constant speed of 10 μm/min. The R-curve was determined from the measurement of crack resistance, $K_{R,}$ as a function of crack extension, Δa. K_R was measured directly for each point of the load-deflection curve from the load by a corrected expression of K_I:[18,19]

$$K_I = HP(a/a_0)^{0.19} \quad (1)$$

where K_I is the stress intensity factor, P is the applied load, H is the geometry and correction factor in DT configuration, and a_0 is the initial crack length.

To avoid an underestimated crack length by the theoretical purely compliance-based method,[20] several crack lengths between 11 and 30 mm (the crack propagation distance in DT specimens) were measured by an optical microscope after the unloading of specimen during the test. These accurate crack lengths were used for correcting and recalculating the crack lengths by:

$$a = \frac{P_f\left(a_f + \frac{D}{B}\right)}{p} - \frac{D}{B}. \quad (2)$$

where a_f and P_f are the values of crack length and the load measured at the end of the test (for each unloading points). D and B are constant dependent on the specimen geometry and material stiffness based on the compliance of DT specimens:

$$C = Ba + D \quad (3)$$

The test details and analysis can be found in Refs. [18–22].

Indeed, it is generally assumed that the compliance is a linear function of the crack length [Eq. (3)]. A theoretical expression for B is:

$$B = \left[\frac{6(1+\nu)W_m^2}{EWT^3\psi(T/W)}\right]. \quad (4)$$

where W_m the distance between two points of flexion (mm), W and T the width and the thickness of specimen respectively, ν the Poisson ration, $t = 2T/W$, and $\Psi(T/W)$:

$$\Psi(T/W) = 1 - 0.6302t + 1.20te^{-\pi/t} \quad (5)$$

3. Results and discussion

3.1. R-Curve determination using the SENB method

The compliance-based calculation of crack length may be not precise and there is a deviation from real crack length in SENB method, due to crack bridging stresses acting to reduce crack opening. Therefore, it is necessary to choose another method for measuring the real crack length. For achieving this purpose, the in situ measurement of crack length during the test was performed on medium-grained and coarse-grained alumina. No correct in situ measurement of crack length as a function of the load could be performed for fine-grained alumina such as SM4, SM8 and AKP6 because of a too important crack speed (unstable crack growth).

Fig. 1 represents the R-curve measured for the medium-grained and coarse-grained alumina ceramics. The real crack resistance curve is obtained by the in situ measurement of the crack length, which gives a rising R-curve from the beginning to the end of the test.

3.2. Compliance analysis

Fig. 2 represents the compliance of DT specimens with successive renotching (from 10 to 30 mm on the same specimen) for the three grain sizes of SM alumina ceramics. The similar results were obtained for AKP alumina ceramics. The results are compared to the slope obtained theoretically by Eq. (4). The experimental results are in good agreement with the analysis, since a notch corresponds exactly to the formation of two almost independent beams, without interaction due to a curved crack front or crack bridging.

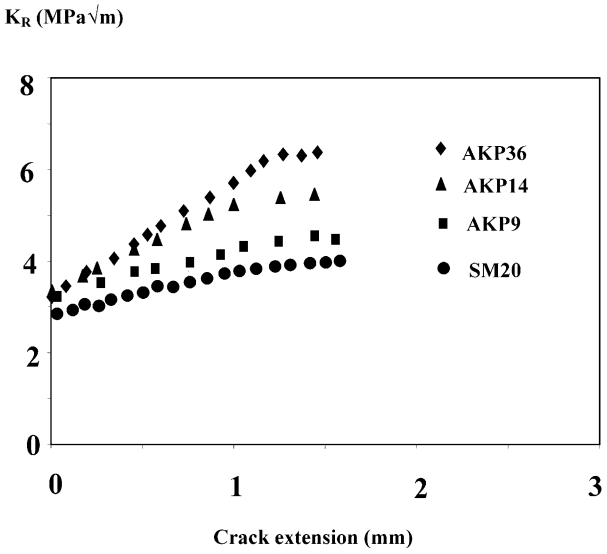

Fig. 1. R-curve (SENB) measured by an in situ measurement of the crack length for the various alumina ceramics.

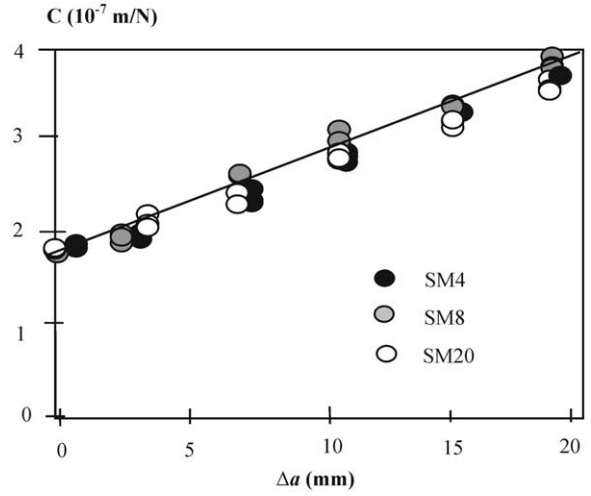

Fig. 2. Compliance obtained from successive renotching of DT specimens for various alumina. Solid line represents the theoretical evolution by Eq. (4).

On the contrary, Fig. 3 shows the evolution of the DT compliance with the real crack extension (from an initial notch length equal to 10 mm) for the various alumina ceramics. As already noticed in the literature, the compliance is not a linear function of the crack length on the overall domain of crack extension, but only between 13 and 30 mm ($\Delta a = 3$–20 mm). The first non linearity observed for small crack length corresponds to the crack initiation which is accompanied by a change of the crack front geometry from straight to curve.[19] Second non linearity for large crack length which was not shown here corresponds to edge effects, as it was described elsewhere.[22] The more important result is that the discrepancy between Eq. (4) and the experiments is higher for the coarser microstructure (AKP36 with a mean grain size of 35.5 μm). This, again, confirms that compliance is affected by bridging interactions behind the crack that act to close the crack. Fig. 3 also shows that the microstructure with elongated grains result in higher discrepancy from solid line compared with the equiaxed grains (compare the results of AKP14 and SM20).

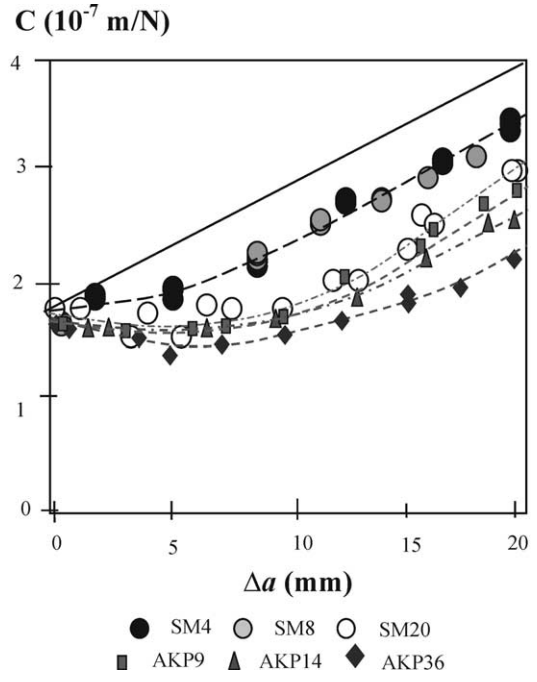

Fig. 3. Compliance of the DT specimen versus crack length (notch: 10 mm) for the alumina ceramics. Solid line represents the theoretical evolution by Eq. (4).

According to a crack bridging analysis[14] based on compliance method, the calculation of bridging-stress/crack opening displacement ($\sigma_b - w$) relationship of a material was proposed by considering the difference between the real compliance of the specimen $C_{(real)}$ and the theoretical compliance $C_{(th)}$, which can be calculated from theoretical purely elastic models or measured with notches. It is argued that because of the effect of bridging stresses on crack opening displacement, $C_{(real)} < C_{(th)}$. This inequality results from crack-interface bridging stresses which cause $C_{(real)}$ to be less than the ideal elastic compliance. In other word, the inequality $C_{(real)} < C_{(th)}$ can provide a measurement of the bridging stress influence. A compliance function, $\phi(\Delta a)$, is defined which increases from zero to a given value and shows a plateau when the bridging zone is fully developed:

$$\phi(\Delta a) = \frac{C_{th}(a)}{\dfrac{\partial C_{th}}{\partial a}} \left(\frac{C_{th}(a)}{C_{real}(a)} - 1 \right). \tag{6}$$

Δa being the crack increment from the notch tip ($a - a_0$). This function is null for ceramics without bridging $C_{(real)} = C_{(th)}$. Ceramics exhibit in many cases a bridging stress function on the form of a power law: [14]

$$\frac{\sigma_b(x)}{\sigma_m} = \left(1 - \frac{w(x)}{w_c}\right)^n \tag{7}$$

where the different parameters are listed in Fig. 4.

It is shown that the compliance function is related to the different bridging parameters by:[23]

$$\begin{cases} \phi(\Delta a) = \dfrac{X}{n+1}\left\{1 - \left[1 - \dfrac{\Delta a}{X}\right]^{n+1}\right\} & \text{for } \Delta a < X \text{ (before fully developed zone)} \\ \phi(\Delta a) = \dfrac{X}{n+1} & \text{for } \Delta a > X \text{ (fully developed zone)} \end{cases} \tag{8}$$

From the knowledge of the compliance function, the parameters of the crack-bridging stresses at the crack

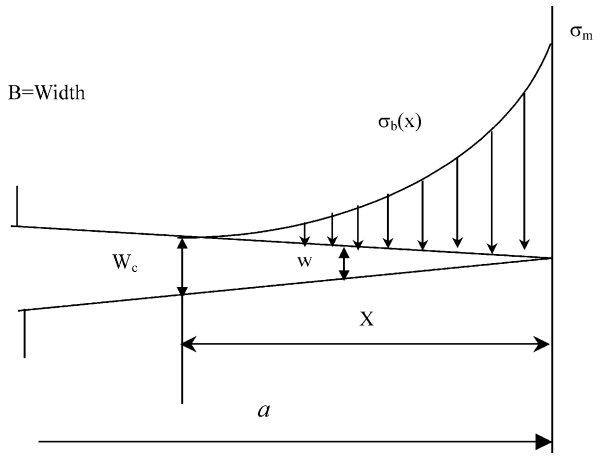

Fig. 4. Power law bridging stress function for a crack with a fully saturated process zone of length X and critical opening displacement W_c.

wake can be obtained, thus to determine the R-curve in any testing configuration from the K-superposition method. In this analysis, it is considered that ϕ-curve and experimental R-curve are proportional.

The $\phi(\Delta a)$ function of various alumina ceramics was calculated from Eq. (6) by using the data of Figs. 2 and 3 (C_{th} and C_{real} functions). The results are shown in Fig. 5 for SM alumina ceramics. The $\phi(\Delta a)$ function increases first, then shows a plateau value for $\Delta a \approx 5$ mm for fine grain SM4 and SM8 alumina ceramics. This first increase of $\phi(\Delta a)$ should be related to the formation of the curved crack front leading to an unbroken ligament in the compression zone. The function increases monotonically with increasing crack length for the coarse grain SM20 alumina with equiaxed grains, in result of an increase of crack bridging zone over several millimeters without saturation and then, it reaches a plateau. The results of theoretical-compliance analysis of DT specimens (dashed line) obtained from $\phi(\Delta a)$ function and the experimental R-curve (solid line) obtained on DT specimen of the same alumina (SM20) are shown in Fig. 5. The $\phi(\Delta a)$ curves obtained from compliance analysis (dashed lines) and the experimental R-curves on DT specimens for various AKP alumina ceramics are shown in Fig. 6. The positive ϕ-curve indicates that the R-curve of coarse-grained alumina is predominately due to crack-interface bridging. The ϕ-curves obtained from the compliance analysis are in good agreement with the experimental R-curves for both alumina ceramics. The results can be also compared with the experimental R-curve obtained by SENB method (Fig. 1). The difference between the R-curves (for instance the results for SM20 alumina: $K_{max} \approx 4$ MPa$\sqrt{m}$ in SENB method compared with $K_{max} \approx 4.5$ MPa$\sqrt{m}$ in DT method) may be related to the low crack extension limit in SENB method (1.5 mm) compared with DT method (20 mm). It means that in SENB method there is not enough crack propagation to reach a plateau during the crack extension. On the other hand the lower rate of crack propagation in DT method results more stability and accuracy in crack propagation results. The results in Figs. 5 and 6 show that compliance analysis can be simple method and powerful tool for accurate R-curve determination.

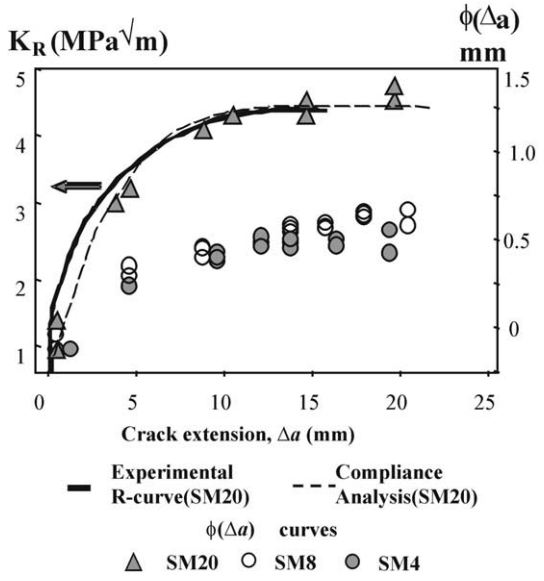

Fig. 5. $\phi(\Delta a)$ functions for SM alumina ceramics. R-curve obtained from compliance analysis (dashed) and experimental R-curve (solid) forSM20 alumina (DT specimens).

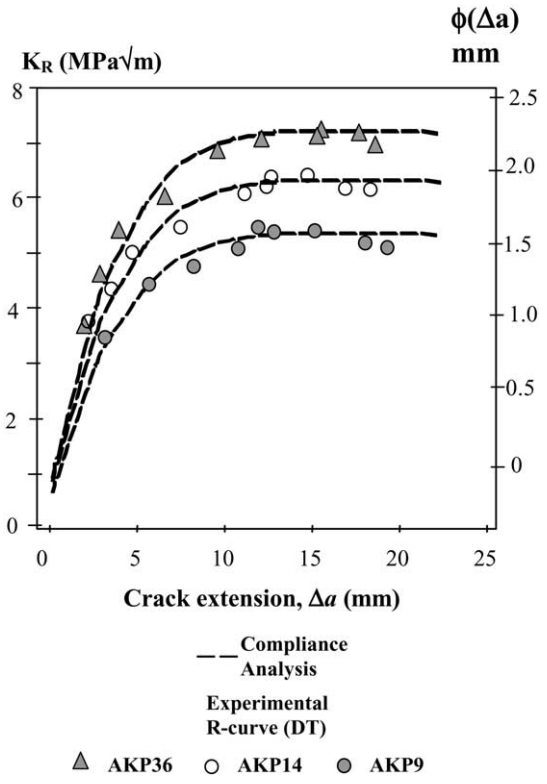

Fig. 6. R-curve obtained from compliance analysis (dashed) and experimental R-curves for AKP alumina ceramics (DT specimens).

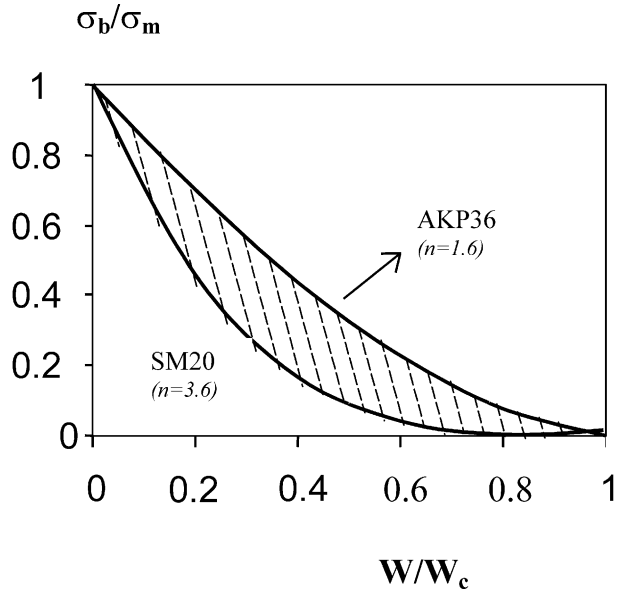

Fig. 7. Bridging-stress distributions of two alumina ceramics.

The ϕ-functions in Fig. 5 show that the compliance of cracked specimens is higher than that of notched specimens ($\phi < 0$) at the very beginning of crack extension (for $a < 2$ mm), although the specimens were previously precracked from the sawcut notch. This is related to the fact that the crack front is not fully established before 5 mm extension. A plateau value of $K_R \approx 4.5$ MPa·m$^{1/2}$ is clearly observed in Fig. 5 for SM20 alumina when the crack extension Δa is higher than 8 mm. The ϕ-curve in the same figure shows a steady increase of ϕ with Δa until a plateau value ($\phi \approx 1.25$ mm) is reached for $\Delta a > 8$ mm. This figure shows that crack bridging has not been established until Δa is about 2 mm from the initial pre-crack. The initial rapid crack extension of nearly 2 mm for DT specimen also confirms this conclusion. Therefore, the fully saturated bridging zone X should be between 5.5 and 6 mm, rather than 7.5 and 8 mm as shown in Fig. 5. Assuming the average $X = 5.75$ mm and $\phi = 1.25$ (plateau) for SM20 alumina, from Eq. (8) we obtain $n = 3.6$ for coarse-grained alumina. n Is a parameter which corresponds to the decline of bridging stress with displacement distance. The n parameters for AKP9, AKP14 and AKP36 were obtained as 2.8, 2.0 and 1.6 respectively. The exponent n of alumina ceramics determined with other methods has been reported. For instance $n \approx 3$ determined from R-curve fitting[10] for an alumina with an average grain size of 16 μm, $n \approx 2.8$ obtained for an alumina with average grain size of 35 μm under monothonic loading,[23] and $n \approx 2.5$ from in -situ scanning electron microscopy measurements of crack profile behind a crack tip for an alumina with an average grain size of 16 μm.[6]

By replacing n in Eq. (7) for various alumina ceramics, bridging-stress distributions were obtained as shown in Fig. 7. The stress distributions of two extreme curves i.e. $n = 1.6$ and $n = 3.6$ for AKP36 and SM20 respectively, are shown in the figure.

4. Conclusion

The SENB and DT test geometries were used to determination of R-curves and compliance measurements for different alumina ceramics.

The compliance is affected by crack bridging elastic ligaments that act to close the crack. This was particularly visible for the coarse-grained alumina ceramics.

A comparison between the compliance of notched and cracked DT specimens was used for prediction of R-curve and determination of bridging-stress distribution for different alumina ceramics. The predicted R-curves obtained by compliance analysis (ϕ-curves) are in good agreement with experimental R-curves of the materials. The n parameter of bridging stress obtained in this analysis is comparable with other methods.

References

1. Hubner, H. and Jillek, W., Subcritical crack extention and crack resistance in polycrystalline alumina. *J. Mater. Sci.*, 1977, **12**, 117–125.
2. Deuerler, F., Knehans, R. and Steinbrech, R. W., Testing-methods and crack resistance behavior of Al_2O_3; in Science in Ceramics 13. *J. Phys. (Paris)*, 1986, C1–617–621.
3. Salem, J. A., Shannon, J. L. Jr. and Bradet, R. C., Crack growth resistance of textured alumina. *J. Am. Ceram. Soc.*, 1989, **72**(1), 20–27.
4. Swain, M. V., *R*-Curve behavior in a polycrystalline alumina materials. *J. Mater. Sci. Lett.*, 1986, **5**, 1313–1315.
5. Swanson, P. L., Fairbanks, C. J., Lawn, B. R., Mai, Y. W. and Hockey, B. J., Crack-interface grain bridging as a fracture resistance mechanism in ceramics: i. experimental study on alumina. *J. Am. Ceram. Soc.*, 1987, **70**(4), 279–288.
6. Rodel, J., Kelly, J. F. and Lawn, B. R., In situ measurements of bridged crack interfaces in the SEM. *J. Am. Ceram. Soc.*, 1990, **73**(11), 3313–3318.
7. Knehans, R. and Steinbretch, R. W., Memory effect of crack resistance during slow crack growth in notched Al_2O_3 bend specimens. *J. Mater. Sci. Lett.*, 1982, **1**(8), 327–329.
8. Fett, T., Determination of bridging stresses and *r*-curves from load-displacement curves. *Engineering Fracture Mechanics*, 1995, **52**(5), 803–810.
9. Fett, T., Influence of Bridging Stresses on Specimen Compliance. *Engineering Fracture Mechanics*, 1996, **53**(3), 363–370.
10. Steinbrech, R. W., Reichl, A. and Schaarwachter, W., *R*-Curve behavior of long cracks in alumina. *J. Am. Ceram. Soc.*, 1990, **73**(7), 2009–2015.
11. Fett, T. and Munz, D., Bridging stress relations for ceramic materials. *J. Eur. Ceram. Soc.*, 1995, **15**, 377–383.
12. Mai, Y. W., Fracture resistance and fracture mechanics of engineering materials. *Mater. Forum.*, 1988, **11**, 232–267.
13. Fett, T., Munz, D., Geraghty, R. D. and White, K. D., Bridging stress determination by evaluation of the R-curve. *J. Eur. Ceram. Soc.*, 2000, **20**, 2143–2148.
14. Hu, X. Z. and Mai, Y. W., Crack-bridging analysis for alumina

ceramics under monotonic and cyclic loading. *J. Am. Ceram. Soc.*, 1992, **75**(4), 848–853.
15. Reichl, A. and Steinbrech, R. W., Determination of crack-bridging forces in alumina. *J. Am. Ceram. Soc.*, 1998, **71**(6), C-299–C-301.
16. Sakai, M., Yoshimura, J. I., Goto, Y. and Inagaki, M., *R*-curve behavior of a polycrystalline graphite: microcracking and grain bridging in the wake region. *J. Am. Ceram. Soc.*, 1988, **71**(8), 609–616.
17. Ebrahimi, M. E., Chevalier, J. and Fantozzi, G., Effect of grain size on crack growth in alumina. In *Fracture Mechanics of Ceramics, Vol. 13*, ed. R. C. Bradt, D. Munz, M. Sakai, V.Ya. Shevchenko and K. W. White. Kluwer Academic/Plenum Publishers, New York, 2002, pp. 273–286.
18. Ebrahimi, M. E., Chevalier, J. and Fantozzi, G., Slow crack-growth behavior of alumina ceramics. *J. Mater. Res.*, 2000, **15**(1), 142–147.
19. Chevalier, J., Saadaoui, M., Olagnon, C. and Fantozzi, G., Double torsion testing a 3Y-TZP ceramics. *Ceram. Int.*, 1996, **22**, 171–177.
20. Ebrahimi, M. E., Chevalier, J. and Fantozzi, G., Compliance and crack-bridging analysis for alumina ceramics. In *Proceedings of the 25th Annual Conference on Composites, Advanced Ceramics, Materials, and Structures: A, Vol. 22*, ed. M. Singh and T. Jessen. The American Ceramic Society, 2001, pp. 277–288.
21. Williams, D. P. and Evans, A. J., A simple method for studying slow crack growth. *Journal of Testing and Evaluation, JTEVA*, 1973, **1**(4), 264–270.
22. Plekta, B. J., Fuller, E. R. and Koepke, B. G., Fracture mechanics applied to brittle materials. *Proceedings of the 11th Symposium on Fracture Mechanics Part II*, 1979, **66**, 19–38.
23. Hu, X. and Mai, Y. W., Compliance analysis of a bridged crack under monotonic and cyclic loading. *J. Eur. Ceram. Soc.*, 1992, **9**, 213–217.